Study of optical phonon lifetimes near the diffuse phase transition in relaxor ferroelectric thin films

2008 J. Phys.: Condens. Matter 20 125211

(http://iopscience.iop.org/0953-8984/20/12/125211)

J. Phys.: Condens. Matter **20** (2008) 125211 (7pp) doi:10.1088/0953-8984/20/12/125211

Study of optical phonon lifetimes near the diffuse phase transition in relaxor ferroelectric thin films

Margarita Correa[1], Ashok Kumar[1], R S Katiyar[1,3] and J F Scott[2]

[1] Department of Physics, University of Puerto Rico, San Juan, PR 00931-3343, USA
[2] Centre for Ferroics, Earth Sciences Department, University of Cambridge, Cambridge CB2 3EQ, UK

E-mail: rkatiyar@uprrp.edu

Received 18 December 2007, in final form 3 February 2008
Published 27 February 2008
Online at stacks.iop.org/JPhysCM/20/125211

Abstract

We have studied the lattice dynamical properties of oriented $Pb(Sc_{0.5}Nb_{0.25}Ta_{0.25})O_3$ (PSNT) thin films by micro-Raman spectroscopy in the temperature range of 80–450 K. An anomalous temperature dependence of the integrated intensity and Raman linewidths was found near the diffuse phase transition. The phonon lifetime analysis indicates strong damping of A_{1g} mode phonons near the transition. This analysis falls into two regimes: below the transition an increase in the lifetime with very small activation energy ($E_a \sim 0.001$ eV) is found, and above the transition an increase in the lifetime with higher activation energy ($E_a \sim 0.018$ eV) is fitted. Although the activation energy calculated from the dielectric loss spectra matched within a factor of 3 with the phonon lifetime energy calculations at all temperatures, we interpret these data as non-equilibrium phenomena due to a relaxation bottleneck in a glassy system (Littlewood and Rammal 1988 *Phys. Rev.* B **38** 2675). Whenever activation energy $E \ll kT$ is fitted, one should suspect such processes, and they are known in polyvinylidene fluoride (Zhang 1998 *Science* **280** 2101; Scott 2006 *J. Phys.: Condens. Matter* **18** 7123). The new data provide a new way of characterizing non-equilibrium processes in relaxors.

1. Introduction

Among ferroelectric (FE) materials, relaxors are known to have remarkably high dielectric and piezoelectric properties [1, 2] with a diffuse phase transition and at least partially disordered structure. Due to configurational disorder the properties of relaxors are very different from normal ferroelectrics. Initially it was believed that this unusual dielectric behavior was due to compositional fluctuations. Later it was found that relaxor ferroelectrics (RFE) possess local order of nano-domains in the range of 2–10 nm, which play a crucial role in their lattice dynamics [3–5]. These nano-domains (short-range order) can be transformed into long-range order by application of external electric fields or variation of composition. In particular, the nano-domain reorientation induces polar–strain coupling which makes RFE potential materials for the next generation of MEMS devices. Among relaxors, $PbSc_{0.5}Nb_{0.5}O_3$ (PSN) and $PbSc_{0.5}Ta_{0.5}O_3$ (PST) are of special interest because the degree of structural order of the B-site cations (Sc/Nb/Ta) is dependent upon thermal processing [6, 7] and the relaxor properties closely depend on the degree of order/disorder in the sample [8].

The study of lattice dynamics is a suitable tool to investigate the nature of the RFE state. In general, relaxors transform from a parelectric phase to a ferroelectric phase via first-order phase transitions. Some of the relaxors (like PST) show structural instability, which influences the lattice dynamics [4]; in others (like $PbMg_{1/3}Nb_{2/3}O_3$ (PMN)) it is suppressed but can be realized by application of an external electric field. Most of the lattice dynamical studies have been carried out on PMN, $PbMg_{1/3}Ta_{2/3}O_3$ (PMT), PMN-PT ($PbTiO_3$), and PST solid solutions. In the present investigation the frequencies and assignment of Raman active modes matches well with the earlier lattice dynamical reports for PSN and PST single crystals [9, 10].

The studies of dielectric anomalies and the effect of Ta/Nb substitution on the ferroelectric phase transition and

[3] Author to whom any correspondence should be addressed.

order–disorder phase transition temperature in PSN, PST and PSN–PST single crystals and polycrystalline ceramics were reported earlier [11–14]. In thin films the presence of surfaces, interfaces, size of the nano-islands, film thickness and interfacial strain effects play crucial and decisive roles in influencing their physical properties. For instance, relaxor thin films have lower dielectric constants, stronger frequency dependence, and a large shift of dielectric maximum temperature (T_m) compared with the bulk samples [15, 16]. From the application point of view, the material must be prepared in thin-film forms for possible integration into different devices.

Several attempts that have been carried out for the search of soft modes in complex relaxor perovskites [17]. There is considerably less information on the behavior of optical phonons in the vicinity of the diffuse phase transition. In what follows we report the room temperature polarized Raman spectra and the temperature-dependent unpolarized Raman spectra of highly oriented PSNT thin films in order to obtain data on the behavior of optical phonons. The dielectric relaxation phenomena of thin films were characterized over a wide range of temperature and frequency with special attention near T_m.

2. Experimental details

The $Pb(Sc_{0.5}Nb_{0.25}Ta_{0.25})O_3$ (PSNT) thin films were grown on MgO substrates by pulsed laser deposition techniques; details of the growth process have been described elsewhere [15]. The thickness of the reported PSNT films and the LSCO layer were estimated from the TEM cross-sections of the thin films and were found to be 240 and 80 nm respectively. The details of the dielectric measurements were described elsewhere [14]. The Raman measurements were performed in the backscattering geometry using a Jobin-Yvon T6400 Triplemate instrument. Radiation at 514.5 nm from a Coherent Innova 99 argon laser was focused to about a 2 μm-diameter area by using a Raman microprobe with a 50× objective. A charge-coupled device (CCD) system collected and processed the scattering light. The integration time of the spectrum and the slit width and laser beam power were adjusted in order to have a high signal to noise ratio. The typical spectral resolution for the Raman system with an 1800 grooves mm^{-1} grating and 1 in CCD was less than 1 cm^{-1}. The system was calibrated by Si spectra at room temperature before and after recording the film spectra. The sample was held in a closed cycle LN_2 cryostat (or furnace) and the temperature was controlled from 80–650 K. The temperature stability was within ±1 K during the measurements. The light scattered with geometries $Z(XX)\overline{Z}$ and $Z(XY)\overline{Z}$ were collected with X, Y, and Z axes being the crystallographic a, b, c axes.

3. Raman analysis

The phase diagram of $PbSc_{0.5}Nb_{(1-x)/2}Ta_{x/2}O_3$ ceramics [14] as a function of Ta concentration is shown in figure 1. It indicates that $x = 0.5$ is the cross-over concentration from relaxor ferroelectric (RFE) to diffuse phase transition (DPT) in ferroelectric PSNT. It also indicates that with $x = 0.50$ PSNT will be a suitable material for the investigation of optical phonon anomalies in the vicinity of the relaxor-to-ferroelectric transition, which is a diffuse phase transition. From the phase diagram we observe that the phase transition of this composition is very near room temperature, which makes it suitable for device applications. The PSNT ceramics show a diffuse phase transition with $x = 0.5$ but the oriented thin films of the same composition show relaxor behavior with wide diffuse phase transitions. Moreover, the oriented films showed the lowering of dielectric maxima towards the lower temperature which is due to the in plane strain in the films [13, 14]. We concentrated our studies on the optical phonons in PSNT thin films due to the peculiar properties of the observed relaxor behavior and the diffuse dielectric maxima.

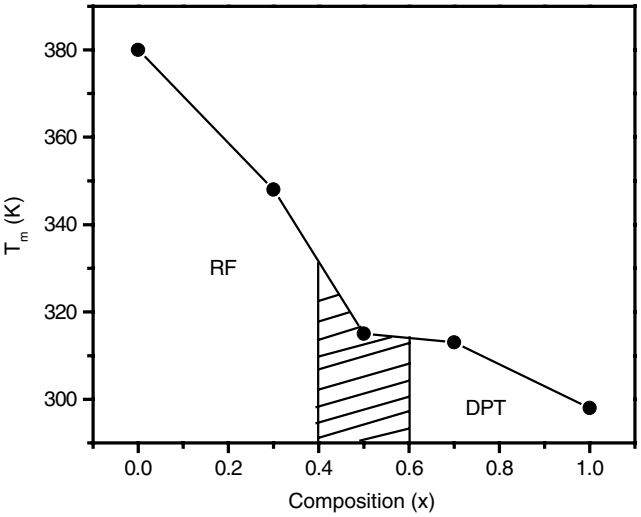

Figure 1. Phase diagram of $Pb(Sc_{0.5}Nb_{0.5-x/2}Ta_{x/2})O_3$ bulk as a function of dielectric maxima temperature.

Figure 2 shows the room temperature polarized Raman spectra of highly oriented thin films. The unpolarized micro-Raman spectra of thin films and the target (used for making the films) were also included for comparative study. The bulk spectra consisted of four major Raman modes with characteristic frequencies 54, 133, 360, and 819 cm^{-1}. The unpolarized Raman spectra for the thin films matched quite well with that in bulk, although the film peak frequencies exhibited a small shift towards lower frequencies. Assuming the average symmetry of the ordered regions as $Fm3m$, the off-diagonal $Z(XY)\overline{Z}$ spectra consist of the F_{2g} Raman active mode with characteristic frequency ∼47 cm^{-1}. As observed in the target, a second F_{2g} mode occurs at ∼360 cm^{-1}; but this mode is masked by the IR active F_{1u} band centered at ∼270 cm^{-1}. Because the F_{2g} symmetry is related to the motion of Pb and O atoms, its linewidth and intensity have been correlated with the coherence length of the order regions in the material [9]. Since this mode (at ∼360 cm^{-1}) is missing (or so diminished in intensity that it is hidden) in the film, we can infer a shorter coherence range in the dipole arrangement in thin films. The dipole arrangement and the size of the nano-ordered regions affect the dielectric response of the samples.

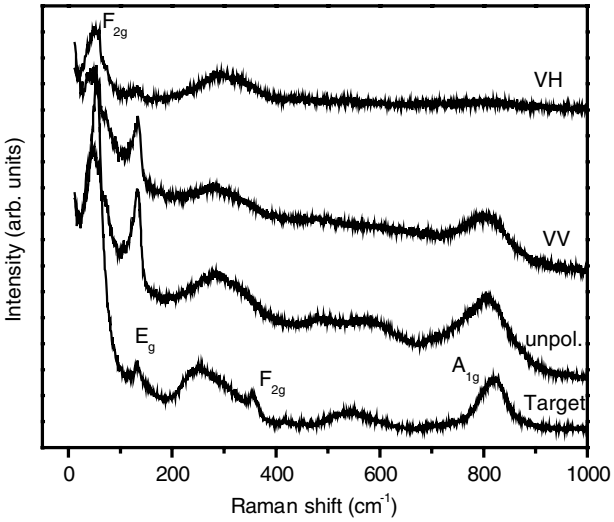

Figure 2. Room temperature Raman spectra of PSNT (a) target used for making the films; (b) unpolarized spectra of PSNT thin films; (c) diagonal $Z(XX)\overline{Z}$ spectra (VV) and (d) off-diagonal $Z(XY)\overline{Z}$ spectra (VH) respectively.

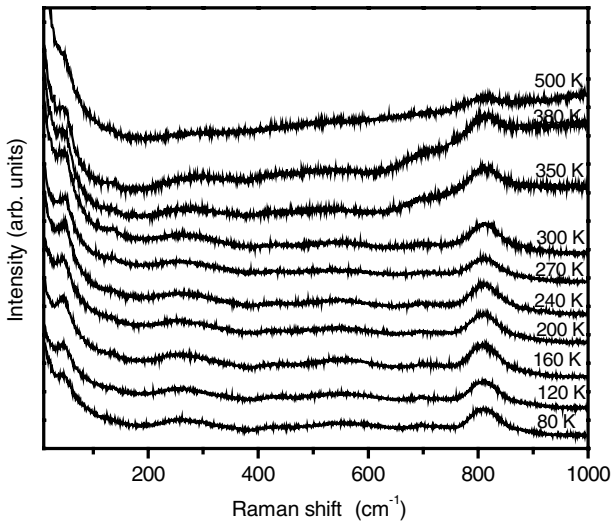

Figure 3. Temperature-dependent Raman spectra of PSNT thin films.

In the bulk samples in which larger coherence lengths were found, PSNT shows normal ferroelectric behavior with no frequency dispersion [14], whereas thin films of the same composition exhibited relaxor behavior [15]. The diagonal $Z(XX)\overline{Z}$ spectra have two Raman active modes at ∼130, and ∼800 cm^{-1}. The higher frequency peak was assigned to the A_{1g} mode, and it represents a breathing-type motion of oxygen ions around the B-site octahedral position. The temperature variation of Raman spectra indicated strong phonon anomalies near the diffuse phase transition. The integrated intensity of A_{1g} modes increased with increase in temperature from 100 K and reached a maximum intensity slightly above the diffuse phase transition, then decreased with further increase in temperature. The integrated intensity of the F_{2g} mode decreases with increase in temperature and becomes perturbed around the diffuse phase transition.

The experimental results were analyzed by integrating reduced Raman scattering intensity given by

$$I_{\text{int}} = \int_{\omega_1}^{\omega_2} I/[n(\omega) + 1]\,\mathrm{d}\omega \qquad (1)$$

where ω_1 and ω_2 are the boundaries of Raman bands and $n(\omega)$ is the Bose population factor. The integrated intensity is proportional to the dielectric anomaly of the related modes through the fluctuation-dissipation theorem. This approach is more relevant for the analysis of temperature evolution of Raman spectra whose linewidths are considerably distorted and damping is high. This approach was successfully used for the Raman measurements of the distorted perovskites $KTa_{1-x}Nb_xO_3$ [18] and $PbMg_{1/3}Ta_{2/3}O_3$ [19]. It is simple to calculate the integrated intensity of A_{1g} modes, because they are well isolated from the other Raman active vibrations. The situation for F_{2g} modes is considerably more complicated due to their diffuse character and their proximity to other vibrations.

Temperature-dependent micro-Raman spectra of PSNT thin films are shown in figure 3. The low-frequency spectrum of symmetry F_{2g} is associated with Pb–O stretching; the mid-frequency regions 200–400 cm^{-1} are of special interest for probing of the ferroelectric change which is often associated with the variation of BO_6 octahedra; and the most striking feature arises from the highest wavenumber mode for probing of relaxor properties whose line shape depends on the compositional variation of B-site elements or local polar nano regions [20]. The most important features observed in the temperature-dependent Raman spectra of PSNT thin films are:

(i) the presence of all Raman active modes well above the DPT temperature;
(ii) a decrease in the integrated intensity of the F_{2g} modes and their perturbation near the DPT transition temperatures;
(iii) the A_{1g} mode showing almost constant intensity down to the freezing temperature ($T_f \sim 180$ K) but increasing from T_f to well above the DPT maxima temperature;
(iv) further decrease in A_{1g} mode intensity around 375 K giving luminescence in the higher frequency regions between 350 and 450 K;
(v) observation of very weak intensity of Raman active modes near the Burns temperature ($T_d \sim 545$ K).

We have not observed softening in the lowest frequency vibrational modes.

We discuss the above observations in the context of oscillator fitting of F_{2g} and A_{1g} modes. Figure 4(a) shows a decrease in integrated intensity of the F_{2g} mode (open circles) up to 200 K; later in the temperature regions of dielectric dispersion the intensity of this phonon mode becomes perturbed (an increase very near the transition temperature presumably due to fluctuations), followed by a decrease in the intensity with further increase in temperature. This behavior corresponds to the relaxor ferroelectric phase transition. A broad dielectric anomaly of PSNT thin films was also found in the same temperature region. The temperature

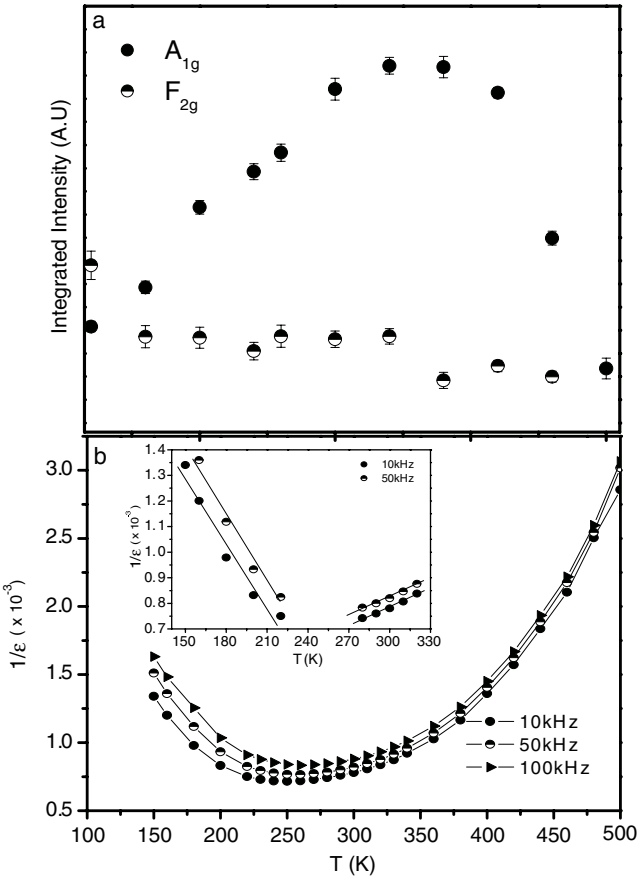

Figure 4. (a) Integrated intensity of A_{1g} and F_{2g} modes of PSNT thin films over a wide range of temperature. (b) Inverse of dielectric constant as a function of temperature and their slope above and below diffuse phase transition temperature (inset).

variation of the integrated intensity of A_{1g} mode shows an anomaly near the diffuse phase transition temperature. The intensity of the A_{1g} mode started to increase on heating at 175 K and reached a maximum in the region of the diffuse phase transition, well above T_m, and then further decreased in intensity with increase in temperature. In the absence of any soft mode anomaly, we expect a change in integrated intensity of the hard modes in Raman spectra in the vicinity of the phase transition [20, 21], especially for relaxor materials. As expected, we observed a perturbation in F_{2g} modes near the diffuse phase transition; but the hard mode (A_{1g}) phonon anomaly is mainly due to the different type of interaction and the compositional fluctuations at the B-site in the temperature regime of the broad dielectric dispersion. The observation of luminescence may be due to the growth of oxygen vacancies, enhancement in inhomogeneous strain, defects at the octahedra positions, growing or merging of polar micro regions. Oxygen vacancies are the most common point defects in titanates [22]. These defects may create some metastable energy state in the band gap which causes luminescence. A similar luminescence feature was observed in PMN by Flerova *et al* [23] and Meng *et al* [24]. The impedance spectra of PSNT thin films show a drastic change in the impedance around 350 °C. It shows negative temperature resistance of coefficient (NTCR) behavior. The observation of luminescence needs further study to find the proper cause of luminescence between T_m and the Burns temperature (T_d).

Figure 4(b) shows the inverse dielectric permittivity of the PSNT thin films. We analyzed our Raman data in the vicinity of the inverse dielectric response. We observed an anomaly in the hard modes (A_{1g}) in the dispersive regions of the dielectric spectra. It indicated perturbation of F_{2g} modes in the dispersive regions followed by a step decrease in the integrated intensity. These observations can be explained on the basis of relaxation process in the polar nano (local) regions that provide dielectric dispersion, responsible for the anomalous behavior of the hard modes. The shape of high-frequency A_{1g} mode indicates significant temperature evolution. Figure 4(b) (inset) gives the slope of the inverse of dielectric permittivity well above and below dielectric maximum temperature. The calculated value of the slope is 4.5:1. Unfortunately only strain-free models [25–27] predict slope ratios of 2:1 for second-order transition whereas these models do not predict the perfect slope for first-order transition. As we know, for first-order transitions the ratio is not 4:1 or 6:1 or 8:1, but in general when strain is included, the ratio is not even an integer. Purely second-order displacive transitions often have ratios of order 4.5:1 due to strain coupling [27–30]. The slope of the inverse of dielectric permittivity therefore does not itself imply an order–disorder transition nor discriminate between first-order and second-order transformations.

4. Phonon lifetimes

An optical mode can interchange energy with other lattice modes due to anharmonicity of the lattice forces and in this way maintain thermal equilibrium energy content. The relaxation time of the optical modes, however, behaves the same way as the line width in Raman scattering, in infrared absorption and in inelastic neutron scattering. The phonon lifetime τ can be derived from the Raman spectra via energy–time uncertainty relation [31–33]

$$\frac{1}{\tau} = \frac{\Delta E}{\hbar} = 2\pi c\Gamma \qquad (2)$$

ΔE is the uncertainty in the energy of the phonon mode; Γ, the full width at half maxima (FWHM) of the Raman peak (cm^{-1}); and $\hbar$, Planck's constant.

The phonon lifetime is mainly limited due to anharmonic decay of a phonon into two or more phonons so that the energy and the momentum are conserved with a characteristic decay time τ.

Figure 5(a) shows the relaxation time as function of inverse temperature, calculated from the line shape (FWHM) of A_{1g} mode as shown in the inset. The relaxation time decreases with decrease in temperature, making a 'U-shape' near the diffuse phase transition and increasing further with decrease in temperature, almost constant far below the glass transition temperature. The relaxation time characteristic of A_{1g} hard mode phonon is related to the 'waterfall' behavior investigated by the inelastic neutron scattering for relaxor materials [17, 34]. These data indicate that the lattice dynamics of PSNT are intimately connected with the condensation of polar nano regions (PNR) at T_f causing a diffuse phase

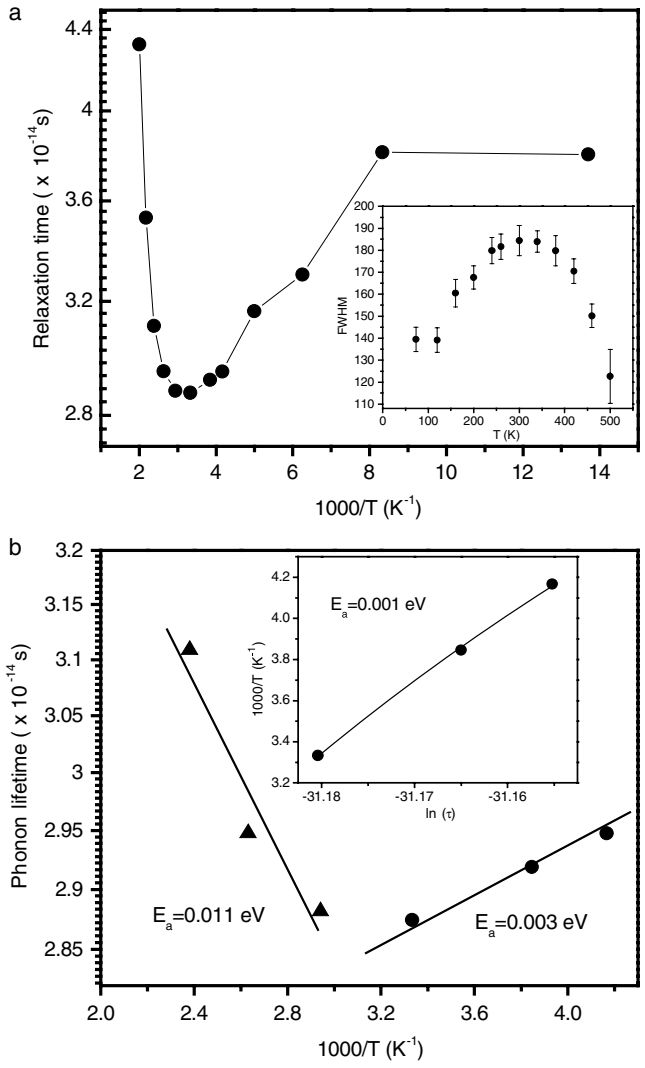

Figure 5. (a) Relaxation time A_{1g} mode of PSNT thin films as function of inverse temperature and line shape (FWHM) as a function of temperature (inset). (b) Phonon lifetime behavior of A_{1g} mode and its linear and nonlinear fitting (inset) with activation energy near diffuse phase transition.

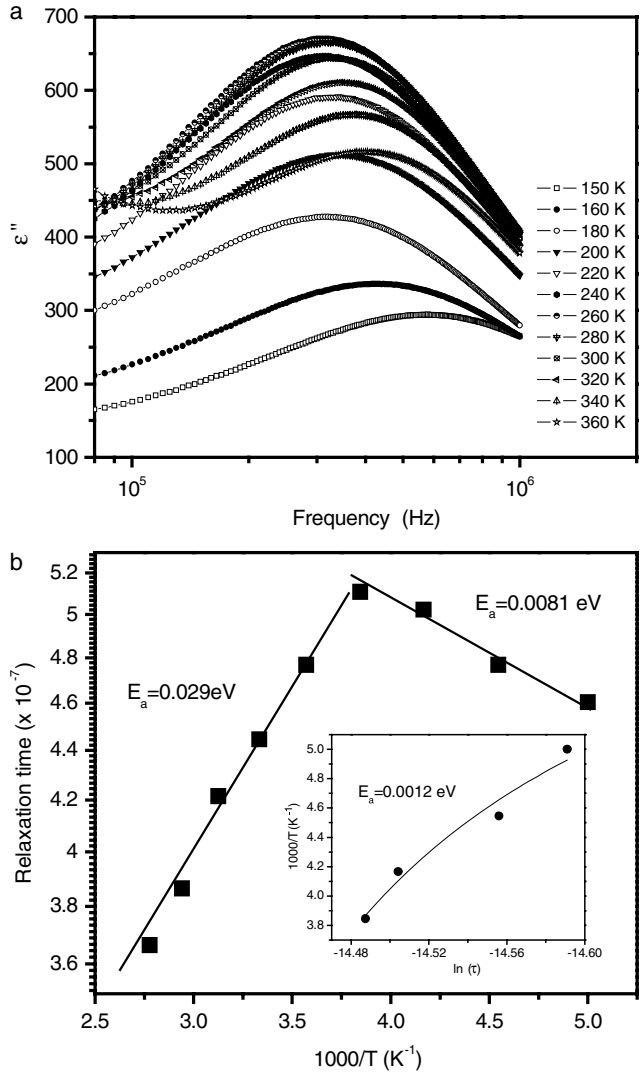

Figure 6. (a) Dielectric loss spectra as a function of frequency over a wide range of temperature. (b) Relaxation time as a function of temperature and linear and nonlinear fitting (inset) to get activation energy near diffuse phase transition.

transition T_m. The over-damping of the optical phonons near the diffuse phase transition is due to the polar nano regions. Wakimoto *et al* observed similar features for the soft mode in PMN by inelastic neutron scattering [34]. Arrhenius (linear) and Vogel–Fulcher (VF) (nonlinear) fitting were carried out for the calculation of relaxation time (τ) and the activation energy [28]. The activation energy calculated from the linear fitting of phonon relaxation time: $\tau = \tau_0 \exp(-E_a/k_B T)$. The calculated values are $E_a = 0.003$ eV and $E_a = 0.011$ eV below and above the diffuse phase transition temperature respectively. We also calculated the activation energy from the nonlinear fitting of the phonon relaxation time between T_f and T_m using Vogel–Fulcher relation [35].

$$\tau = \tau_0 \exp\left(E_a/k_B(T_m - T_f)\right)$$

where, τ is the experimental frequency, τ_0 is the pre-exponential factor, E_a is the activation energy, k_B is the Boltzmann constant and T_f is the static freezing temperature.

The value of the activation energy calculated from the nonlinear fitting is 0.001 eV (1 ± 1 meV), which is of the same order of magnitude as calculated from the linear fitting of 0.003 eV (3 ± 1 meV). We used the same data for linear and nonlinear fitting due to the small temperature regions between T_f and T_m. The value of the activation energy for the polar nano regions (between T_f and T_m) is one order less than the activation energy above T_m.

We correlated our phonon data to the dielectric loss anomaly (figure 6(a)) over a wide range of temperature and frequency. We observed a significant change in the dielectric loss peaks near the diffuse phase transition. We calculated the relaxation time from the inverse of dielectric loss peaks using universal equation $\omega_{max}\tau = 1$ that is independent of geometrical factors. Note that $\tau(T)$ is strongly temperature-dependent. The linear fitting of the relaxation time, calculated from the dielectric loss spectra, is shown in figure 6(b). The activation energy calculated from the loss spectra is $E_a = 0.008$ and 0.029 eV below and above the diffuse phase

transition temperature respectively. These values agree only within a factor of 3 with the activation energy calculated from the phonon lifetimes, in each case being 3× larger. Figure 6(b) (inset) shows the nonlinear fitting of the relaxation time calculated from the dielectric loss spectra. The value of the activation energy is 0.002 eV and matches well with the nonlinear fitting and energy calculation of the phonon lifetime.

What do these activation energies mean? We argue that they mean nothing at all! Whenever one fits data to activation energy E_a that is less than kT, one should be very suspicious. Arrhenius models assume thermal equilibrium, but generally systems with apparent activation energies $E_a < kT$ are not in thermal equilibrium. Instead the fitted activation energy is a non-equilibrium artifact that arises from a relaxation bottleneck. As shown by Littlewood and Rammal [36], such bottlenecks usually arise in glasses, and hence the present result is a new way of characterizing the glassy behavior of a relaxor. Of course this is compatible with Vogel–Fulcher modeling of the data, as well. Similar data with $E_a \ll kT$ have been reported by Zhang for polyvinylidene fluoride [37].

5. Conclusions

In summery, lattice dynamical studies of PSNT thin films were carried out in the vicinity of the diffused phase transition region. We observed almost no change in the integrated intensity of F_{2g} and A_{1g} modes below T_f but merely small perturbations of the F_{2g} mode frequencies and scattering intensities; an anomalous behavior of A_{1g} modes was seen near the DPT. The slope of the inverse of dielectric permittivity below and above DPT is 4.5:1 typical of that for second-order transitions with strain coupling [27]. We observed damping of the phonon lifetime near DPT. The activation energy calculated between T_m and T_f by both dielectric and phonon lifetime fitting is an order of magnitude less than the activation energy above T_m, perhaps due to active polar nano regions between T_m and T_f; but we emphasize that these 'activation energies' are $<kT$ and most probably due to non-equilibrium glassy relaxation bottlenecks, as in PVDF experiments [37] and the theory of Littlewood and Rammal [36]. This is not disappointing, as it gives us new insight into the non-equilibrium glassy behavior of relaxors. The phonon lifetime characteristics of A_{1g} hard mode phonon are analogous to the 'waterfall' behavior investigated by inelastic neutron scattering for relaxor materials. The activation energy calculated from the dielectric loss spectra matched within ×3 and supported the phonon lifetime observation, although neither seems to be a true equilibrium value. The idea that relaxors are not in thermal equilibrium has been stressed elsewhere in the context of critical exponents. It has been shown that relaxors take a very long time (hours or even days) to equilibrate at temperatures near their phase transitions: see Weissman [38], Chao *et al* [39], or Scott [40].

Acknowledgments

We acknowledge support for NASA, Center for Nanoscale Material Grant No. NCC3-1034 and NSF Grant NSF-0305588. One of us (Margarita Correa) also acknowledges NSF-IFN sponsored graduate fellowship.

References

[1] Cross L E 1987 *Ferroelectrics* **76** 241
[2] Fu H and Cohen R E 2000 *Nature* **403** 281
[3] Burns G and Dacol F H 1983 *Solid State Commun.* **48** 853
[4] Smolenskii G A *et al* 1984 *Ferroelectrics and Related Materials* (New York: Gordon and Breach)
[5] Siny I G and Boulesteix C 1989 *Ferroelectrics* **96** 119
[6] Stenger C G and Burgraaf A F 1980 *Phys. Status Solidi* a **61** 275
[7] Stenger C G and Burgraaf A F 1980 *Phys. Status Solidi* a **61** 653
[8] Randall C A and Bahlla A S 1990 *Japan. J. Appl. Phys.* **29** 327
[9] Siny I G, Katiyar R S and Bhalla A S 1998 *J. Raman Spectrosc.* **29** 385
[10] Siny I G, Katiyar R S and Lushnikov S G 1996 *Proc. XVth Int. Conf. on Raman Spectroscopy* ed S A Asher (New York: Wiley) p 1002
[11] Caranoni C, Menguy N, Hilczer B, Glinchuk M and Stephanovich V 2000 *Ferroelectrics* **240** 241
[12] Raevski I P, Malitskaya M A, Gagarina E S, Smotrakov V G and Eremkin V V 1999 *Ferroelectrics* **235** 221
[13] Chen Z, Setter N and Cross L E 1981 *Ferroelectrics* **37** 619
[14] Correa M, Choudhary R N P and Katiyar R S 2007 *J. Appl. Phys.* **101** 054116
[15] Correa M, Kumar A and Katiyar R S 2007 *Appl. Phys. Lett.* **91** 082905
[16] Catalan G, Corbett M H, Bowman R M and Gregg J M 2002 *J. Appl. Phys.* **91** 2295
[17] Gehring P M, Wakimoto S, Ye Z-G and Shirane G 2001 *Phys. Rev. Lett.* **87** 277601
[18] Fontatana M D, Bouziane E and Kugel G E 1990 *J. Phys.: Condens. Matter* **2** 8681
[19] Lushnikov S, Gvasaliya S and Katiyar R S 2004 *Phys. Rev.* B **70** 172101
[20] Haumont R, Gemeiner P, Dkhil B, Kiat J M and Bulou A 2006 *Phys. Rev.* B **73** 104106
[21] Salje E K H and Bismayer U 1997 *Phase Transit.* **63** 1
[22] Waser R and Smyth D M 1996 *Ferroelectric Thin Films: Synthesis and Basic Properties* ed C P de Araujo, J F Scott and G W Taylor (Amsterdam: Gordon and Breach) p 47
[23] Flerova S A, Krainik N N and Popov S A 1988 *Ferroelectrics* **82** 167
[24] Meng J F, Cheng Z-Y, Rai B K, Katiyar R S, Alberta E, Guo R and Bhalla A S 1988 *J. Mater. Res.* **13** 1861
[25] Huang H, Sun C Q, Tianshu Z and Hing P 2001 *Phys. Rev.* B **36** 184112
[26] Kumar A, Murari N M, Scott J F and Katiyar R S 2007 *Appl. Phys. Lett.* **90** 262907
[27] Errandonea G 1980 *Phys. Rev.* B **21** 5221
[28] Vugmeister B E and Rabitz H 1998 *Phys. Rev.* B **57** 7581
[29] Chu F, Setter N and Tagantsev A K 1990 *J. Appl. Phys.* **68** 2916
[30] Tagantsev A K 1994 *Phys. Rev. Lett.* **72** 1100
[31] Cuscó R, Alarcón-Lladó E, Artús L, Ibáñez J, Jimenez J, Wang B and Callahan M J 2007 *Phys. Rev.* B **75** 165202
[32] Ridley B K and Gupta R 1991 *Phys. Rev.* B **43** 4939
[33] Bergman L, Alexson D, Murphy P L, Nemanich R J, Dutta M, Stroscio M A, Balkas C, Shin H and Davis R F 1999 *Phys. Rev.* B **59** 12977
[34] Wakimoto S, Stock C, Birgeneau R J, Ye Z-G, Chen W, Buyers W J L, Gehring P M and Shirane G 2002 *Phys. Rev.* B **65** 172105
[35] Vogel H 1921 *Z. Phys.* **22** 645

[36] Littlewood P B and Rammal R 1988 *Phys. Rev.* B **38** 2675
[37] Zhang Q M 1998 *Science* **280** 2101
[38] Weissman M B *et al* 2003 *AIP Conf. Proc.* **667** 33
[39] Chao L K, Colla E, Weissman M B and Viehland D 2005 *Phys. Rev.* B **72** 134105
[40] Scott J F 2006 *J. Phys.: Condens. Matter* **18** 7123